Proceedings of ISINN-29, JINR, E3-2023-58, Dubna, 2023, p.247 – 262

The Virtual Character of Spontaneous and Induced (with the Participation of Thermal Neutrons) Ternary Fission of Nuclei with the Emission of Prescission Nucleons and Light Nuclei

S.G. Kadmensky, Ya.O. Otvodenko

Voronezh State University, Voronezh, Russia
E-mail: kadmensky@phys.vsu.ru

1. Introduction

In the field theory virtual reactions and decays, connected with the appearance in their amplitudes of states of intermediate elementary particles, whose momenta and energies are not related by Einstein's relativistic formula and therefore lie outside the mass surfaces of analyzed processes, are well known. Such reactions include, for example, the Compton scattering of γ-quanta by free electrons [1].

The question arises whether there are in nuclear physics the class of virtual decays and reactions associated with the appearance in their amplitudes of virtual intermediate states not only various elementary particles, but also composite atomic nuclei lie outside the mass surfaces of analyzed processes. A positive answer to this question was given on the basis of the generalized approach to the description of multistage decays and reactions in chains of genetically linked nuclei [2–4] using the Feynman diagram technique involving Green's functions of intermediate nuclei. The formation of this class at the first stage was started with two-proton decays of neutron-deficient nuclei, predicted by Goldansky [5], whose characteristics were successfully described using the concept of their virtuality [2–4]. This class was later extended [6–9] to include double β-decays of nuclei whose characteristics are calculated using the weak interaction Hamiltonian in second-order perturbation theory, which leads to the appearance of virtual states of intermediate nuclei. In recent years the characteristics of spontaneous and induced (with the participation of thermal neutrons) ternary and quaternary nuclear fission with the emission of prescission α-particles have been described [10] using the concept of virtuality of these types of fission.

The purpose of this work is to demonstrate the possibility of describing the experimental characteristics spontaneous and induced ternary fission of nuclei with the emission of prescission nucleons and light nuclei ^{2}H, ^{3}H and ^{6}He on the basis of the virtual presentation of these processes.

2. The mechanisms of spontaneous and induced (with the participation of thermal neutrons) binary fission of nuclei

The binary fission of fissile nucleus (FN) (A, Z) is connected with its scission into light (A_L, Z_L) and heavy (A_H, Z_H) fission fragments with close values of charges and masses. The process of this fission can be described on the base of the generalized model of nuclei [11], which simultaneously takes into account the nucleonic and collective modes of nuclear motion taking into account the evolution of shape of FN, described by its collective deformation parameters β_λ, from close to spherical through a prolonged spheroid to a dumbbell-like shape (see Fig. 1.).

Fig. 1. Sequential stages of binary fission of nuclei.

For description of this evolution it can introduced the potential energy of deformation $E(\beta_\lambda)$ of FN by formula:

$$E(\beta_\lambda) = \tilde{E}(\beta_\lambda) + E_{sh}(\beta_\lambda), \tag{1}$$

where $\tilde{E}(\beta_\lambda)$ is the binding energy calculated in the liquid-drop model of the nucleus [12] and $E_{sh}(\beta_\lambda)$ is Strutinsky shell correction [13, 14]. Then the FN deformation potential $V(\beta_\lambda) = E(\beta_\lambda) - E(\beta_{20})$, where β_{20} is quadrupole deformation parameter of ground state of FN, can be represented [11] by Fig. 2.

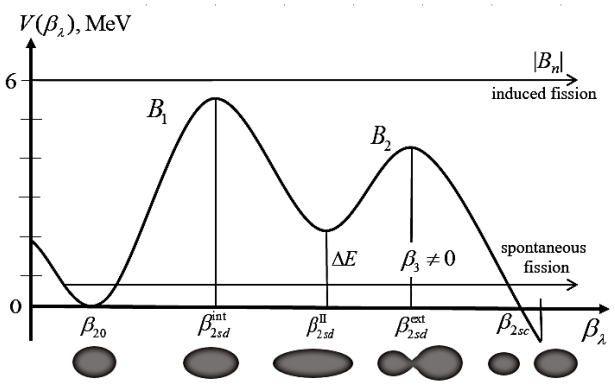

Fig. 2. Deformation potential $V(\beta_\lambda)$ for actinide nuclei

The spontaneous binary fission occurs if FN is in the ground state with the wave function $\psi_{K0}^{JM}(\beta_\lambda)$, where J is FN total spin with its projections M, K, taking into account the zero collective deformation vibration of this nucleus, at which FN passes into the prescission configuration through overcoming the potential deformation barriers shown in Fig. 2. This FN state with wave function $\psi_{K0}^{JM}(\beta_\lambda)$ corresponds to the transition fission state [11] of this nucleus. The binary fission is induced if the compound fissile nucleus (CFN) (A, Z) is formed when capturing of thermal neutron with a very low kinetic energy $T_n \approx 0.025$ eV by target nucleus (A-1, Z) in its ground state with the formation of excited state CFN with the excitation energy $|B_n| \approx 6$ MeV, where B_n is binding energy of captured neutron. For nuclear times $T_0 \approx 10^{-22}$ s this excited state transits into the neutron resonance state of CFN, whose wave function ψ_K^{JM} is represented when using the Wigner random matrix method [15–18] as:

$$\psi_K^{JM} = \sum_{i \neq 0} b_i \psi_{iK}^{JM} + b_0 \psi_{0K}^{JM}(\beta_\lambda). \tag{2}$$

In this formula the wave function ψ_{iK}^{JM} corresponds to the i-quasi-particle excited state of CFN and the wave function $\psi_{0K}^{JM}(\beta_\lambda)$ describes the collective deformation state of the CFN with the excitation energy $|B_n|$ and corresponds to the transition fission state of the CFN [11]. The squares of coefficients b_i and b_0 in (2) have average values of $\overline{(b_i)^2} = 1/N$, where N is the

total number of quasi-particle states participating in formation of wave function (2). The induced fission of CFN occurs with a noticeable probability if the energy $|B_n|$ exceeds heights of the internal and external fission deformation barriers of Fig. 2.

3. The mechanisms of spontaneous and induced (with the participation of thermal neutrons) ternary nuclear fission with the emission of light prescission particles

The spontaneous and induced ternary fission of FN (A, Z) with the emission of third light prescission particle p (A_p, Z_p) is similar to the binary fission of FN beginning with the transition of FN to its prescission configuration shown in Fig. 1. Then particle p flies out of this configuration with the appearance of the state of intermediate nucleus (A-A_p, Z-Z_p), which is further divided into light (A_{LF}, Z_{LF}) and heavy (A_{HF}, Z_{HF}) fission fragments. The angular distribution of particle p for spontaneous and induced ternary fission has anisotropic character with the maximum at emission angles θ_p in the equatorial direction to the direction of light fission fragment emission [19–20], that allows to conclude that the emitted p-particles are formed in the neck of FN prescission configuration. The experimental energy distribution $W(T_p)$ of particle p with kinetic energy T_p have maximum value at energies $T_{p\max}$, which noticeably exceeds the heat Q_p^A of the p-decay of the ground state of FN (A, Z) having the form:

$$Q_p^A = E(A,Z) - E(A-A_p, Z-Z_p) - E(A_p, Z_p), \tag{3}$$

where $E(A,Z)$ is binding energy of FN in liquid-drop model [12]. The indicated fact is serious argument for the justification of the virtual mechanism of the appearance of third light prescission particles p in ternary nuclear fission.

Using the results of works on the theory of virtual decays of atomic nuclei [2–4], can obtain a formula for the width Γ_{pf}^A of the virtual spontaneous ternary fission with the emission of third light particles p:

$$\Gamma_{pf}^{\mathrm{A}} = \frac{1}{2\pi} \int_0^{Q_f^{A-A_p}} \frac{\Gamma_p^{\mathrm{A}}(T_p)\Gamma_f^{(A-A_p)}(Q_f^{A-A_p} - T_p + Q_p^A)}{(Q_p^A - T_p)^2} dT_p \ , \tag{4}$$

where $\Gamma_p^A(T_p)$ is p-decay width of FN (A, Z) with the emission of ternary particle p (A_p,Z_p) in its ground state and the formation of daughter nucleus (A-A_p, Z-Z_p), $\Gamma_f^{(A-A_p)}(Q_f^{A-A_p} - T_p + Q_p^A)$ is full width of binary fission of nucleus (A-A_p, Z-Z_p) with the heat of this fission $Q_f^{A-A_p}$:

$$Q_f^{A-A_p} = E(A-A_p, Z-Z_p) - E(A_{LF}, Z_{LF}) - E(A_{HF}, Z_{HF}). \tag{5}$$

Note that the width of the induced ternary fission of CFN (A, Z) nucleus formed during the capture of a thermal neutron into the ground state of the target nucleus (A-1, Z) is also determined by formula (4), since the CFN excitation energy, equal to $|B_n|$, is conserved in the corresponding prescission configuration of this nucleus and does not participate in the formation of kinetic energy T_p of the p-particle. Now it is possible to introduce the yield of p-particles in ternary nuclear fission to the number of binary fission fragments, defined as $\delta_{pf} = \Gamma_{pf}^{\mathrm{A}} / \Gamma_f^A(Q_f^{A-A_p})$:

$$\delta_{pf} = \frac{1}{2\pi} \int_0^{Q_f^{A-A_p}} \frac{\Gamma_p^{\mathrm{A}}(T_p)\Gamma_f^{(A-A_p)}(Q_f^{A-A_p} - T_p + Q_p^A)}{(Q_p^A - T_p)^2 \Gamma_f^A(Q_f^A)} dT_p \ . \quad (6)$$

From here it is possible to obtain the energy distribution of the emission *p*-particles, normalized on the yield of *p*-particles:

$$W_{pf}(T_p) = \frac{1}{2\pi} \frac{\Gamma_p^{\mathrm{A}}(T_p)\Gamma_f^{(A-A_p)}(Q_f^{A-A_p} - T_p + Q_p^A)}{(Q_p^A - T_p)^2 \Gamma_f^A(Q_f^A)}, \quad (7)$$

normalized to the yield of *p*-particles δ_{pf}. Taking into account that the energy Q_f^{A-4} for actinide nuclei reaches 170 MeV, which is much higher than the energies $T_p - Q_p^A$ and the proximity of the widths $\Gamma_f^{(A-A_p)}(Q_f^{A-A_p})$ and $\Gamma_f^A(Q_f^A)$, formula (7) can be transformed into the form:

$$W_{pf}(T_p) = W_p(T_p) = \frac{1}{2\pi} \frac{\Gamma_p^{\mathrm{A}}(T_p)}{(Q_p^A - T_p)^2}. \quad (8)$$

Hence the value of width $\Gamma_p^{\mathrm{A}}(T_p)$ can be calculated through values $W_{pf}(T_p)$ (8):

$$\Gamma_p^{\mathrm{A}}(T_p) = 2\pi W_p(T_p)(Q_p^A - T_p)^2. \quad (9)$$

The value $\Gamma_p^{\mathrm{A}}(T_p)$ can be represented by Gamow formula:

$$\Gamma_p^{\mathrm{A}}(T_p) = \omega_p \frac{\hbar\sqrt{2T_p}}{2r_{neck}\sqrt{m_p}} P\left(T_p\right), \quad (10)$$

where $P(T_p)$ is the penetrability factor of the Coulomb barrier, close to one for $T_p = T_{p\max}$, m_p is *p*-particle mass and ω_p is the probability of the formation of *p*-particle in the neck of parent nucleus with radius r_{neck}. Using the experimental values of the widths $\Gamma_p^{\mathrm{A}}(T_{p\max})$ and the averaged values of the radii r_{neck} [21], it is possible to calculate by formula (10) the values of ω_p for such third prescission particles *p* as α-particles, protons, neutrons, and also light nuclei ^{2}H, ^{3}H, and ^{6}He, and compare their values with similar values calculated in the framework of the cluster model of the nucleus [22].

4. Spontaneous and induced ternary nuclear fission with the emission of prescission α-particles

When using experimental data for spontaneous (sf) ternary fission with the emission of α-particles from nuclei ^{244}Cm, ^{246}Cm, ^{248}Cm [23] and ^{250}Cf, ^{252}Cf [24] and for analogous induced (n,f) ternary fission of nuclei-targets ^{233}U, ^{235}U [20] and ^{239}Pu, ^{241}Pu [25] the characteristics of these processes were calculated.

As can be seen from Table 1 for all considered CFN the yields of α-particles $\delta_{\alpha f}$ as for spontaneous as well induced fission are close to each other: $1.7\times10^{-3} \le \delta_{\alpha f} \le 3.2\times10^{-3}$. The analogous situation is realized for the probabilities of α-particle formation ω_α: $2.0\times10^{-2} \le \omega_\alpha \le 3.1\times10^{-2}$. The noticeable positive values of differences $(T_{\alpha\max} - Q_\alpha^A)$ show that the analyzed process of ternary fission has the virtual character.

Table 1. Characteristics of spontaneous (sf) and induced (n,f) ternary fission of CFN with the emission of α-particles

Compound nucleus	$\delta_{\alpha f}$ $\times 10^{-3}$		$T_{\alpha\max}$ (MeV)		Q_α^A (MeV)	r_{neck} (fm)	ω_α $\times 10^{-2}$	
	(sf)	(n,f)	(sf)	(n,f)			(sf)	(n,f)
^{244}Cm	3.2	2.4	16.0	16.1	5.9	2.5	3.1	2.6
^{246}Cm	2.5	2.2	16.4	16.4	5.5	2.5	2.8	2.4
^{248}Cm	2.3	1.9	16.0	16.0	5.2	2.5	2.6	2.0
^{250}Cf	2.9	2.8	16.0	16.1	6.1	2.5	2.4	2.6
^{252}Cf	2.6	2.4	16.0	15.9	6.2	2.5	2.4	2.2
^{234}U	-	2.2	-	15.7	4.9	2.5	-	2.9
^{236}U	-	1.7	-	15.5	4.6	2.5	-	2.1
^{240}Pu	-	2.2	-	15.9	5.3	2.5	-	2.4
^{242}Pu	-	1.9	-	15.9	5.0	2.5	-	2.1

As can be seen from Fig. 3 the energy distributions $W_{\alpha f}^A(T_\alpha)$ of α-particles for the spontaneous and induced ternary fission of the CFN ^{252}Cf are close.

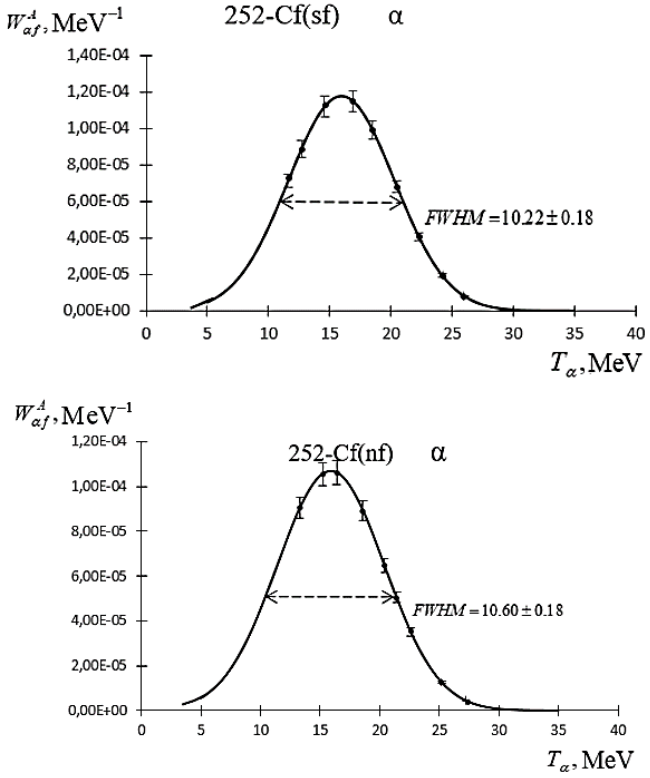

Fig. 3. The energy distributions $W_{\alpha f}^A(T_\alpha)$ for the spontaneous and induced ternary fission of ^{252}Cf with emission α-particle.

From Fig. 3 it can be seen that for both spontaneous and induced fission of CFN with emission α-particle such characteristics as width at half maximum *FWHM* and forms of energy distribution are close.

Similar dependences $W_{\alpha f}^A(T_\alpha)$ are also observed for all CFN of Table 1.

The experimental angular distributions of fragments of ternary fission of FN with emission of α-particles are close to the analogous angular distributions of binary fission fragments due to weak influence of the emitted third α-particle on the angular distributions of ternary fission fragments [18].

The experimental angular distributions of α-particle for all CFN [19–20] have the equatorial character with the maximum close to $\theta = 90°$, what could be related with the emission of α-particle from the neck of the prescission configuration of CFN. Confirmation of this fact can be found in [26] for the spontaneous fission of the ^{252}Cf nucleus.

5. Spontaneous and induced ternary nuclear fission with the emission of prescission ^{1}H

When using experimental data for spontaneous (sf) and induced (n,f) ternary fission with the emission of *p*-particle as ^{1}H from CFN nuclei ^{252}Cf [27] and ^{236}U [28] the characteristics of these processes were calculated.

Table 2. Characteristics of spontaneous (sf) and induced (n,f) ternary fission of CFN with the emission of ^{1}H

Compound nucleus	δ_{pf} ×10^{-5}		$T_{p\max}$ (MeV)		Q_p^A (MeV)	r_{neck} (fm)	ω_p ×10^{-4}	
	(sf)	(n,f)	(sf)	(n,f)			(sf)	(n,f)
^{252}Cf	4.6	-	7.8	-	–6.48	2.5	8.1	-
^{236}U	-	4.0	-	8.6	–6.71	2.5	-	7.6

As can be seen from Table 2 for all considered CFN the yields δ_{pf} of ^{1}H are close to each other as for spontaneous as well induced fission: $4.0\times10^{-5} \le \delta_{pf} \le 4.6\times10^{-5}$. The analogous situation is realized for the probabilities of ^{1}H formation ω_p: $7.6\times10^{-4} \le \omega_p \le 8.1\times10^{-4}$. The noticeable positive values of differences $(T_{p\max} - Q_p^A)$ show that the analyzed process of ternary fission has the virtual character.

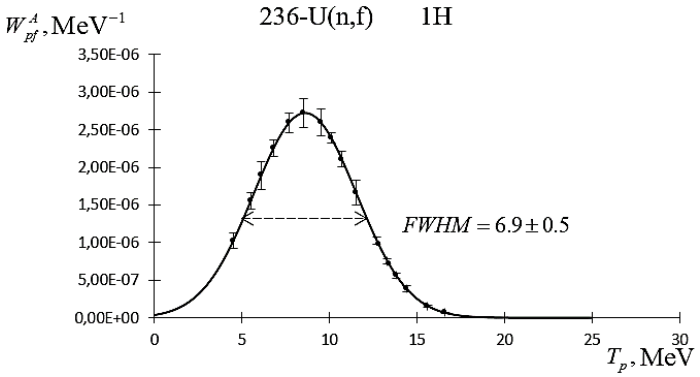

Fig. 4. The dependence $W_{pf}^A(T_p)$ for the induced fission of the compound nucleus ^{236}U with emission ^{1}H.

As can be seen from Figs. 4–5 the dependences $W_{pf}^A(T_p)$ from T_p for the spontaneous and induced ternary fission of the compound nuclei ^{236}U and ^{252}Cf with emission ^{1}H turn out to be close for all CFN considered.

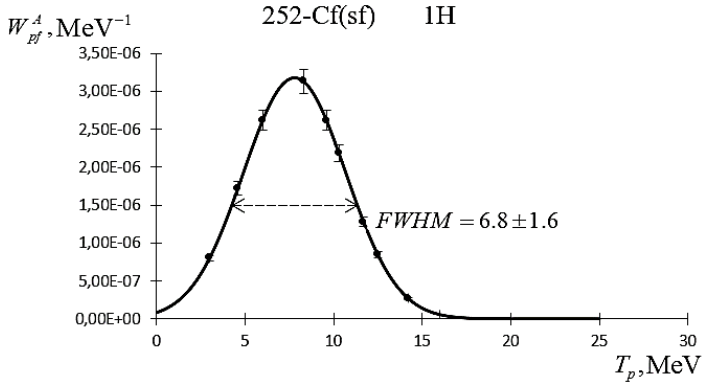

Fig. 5. The dependence $W_{pf}^{A}(T_p)$ for the spontaneous fission of the compound nucleus ^{252}Cf with emission ^{1}H.

As can be seen from Figs. 4–5 the dependences $W_{pf}^{A}(T_p)$ from T_p for the spontaneous and induced ternary fission of the compound nuclei ^{236}U and ^{252}Cf with emission ^{1}H turn out to be close for all CFN considered.

From Figs. 4–5 it can be seen that for both spontaneous and induced fission of CFN with emission ^{1}H such characteristics as width at half maximum *FWHM* and forms of energy distribution are close.

The experimental angular distributions of ^{1}H for all CFN [19–20] have the equatorial character with the maximum close to $\theta =$ 90°, what could be related with the emission of ^{1}H from the neck of the prescission configuration of CFN. Confirmation of this fact can be found in [27] for the spontaneous fission of the ^{252}Cf nucleus.

6. Spontaneous and induced ternary nuclear fission with the emission of prescission ^{2}H

When using experimental data for spontaneous (sf) and induced (n,f) ternary fission with the emission of *p*-particle as ^{2}H from CFN nuclei ^{252}Cf [27] and ^{236}U [28] the characteristics of these processes were calculated.

Table 3. Characteristics of spontaneous (sf) and induced (n,f) ternary fission of CFN with the emission of ^{2}H

Compound nucleus	δ_{pf} ×10^{-5}		$T_{p\max}$ (MeV)		Q_p^A (MeV)	r_{neck} (fm)	ω_p ×10^{-4}	
	(sf)	(n,f)	(sf)	(n,f)			(sf)	(n,f)
^{252}Cf	1.5	-	8.0	-	–9.3	2.5	5.0	-
^{236}U	-	1.2	-	7.9	–10.1	2.5	-	4.5

As can be seen from Table 3 for all considered CFN the yields δ_{pf} of ^{2}H are close to each other as for spontaneous as well induced fission: $1.2\times10^{-5} \le \delta_{pf} \le 1.5\times10^{-5}$. The analogous situation is realized for the probabilities of ^{2}H formation ω_p: $4.5\times10^{-4} \le \omega_p \le 5.0\times10^{-4}$. The noticeable positive values of differences $(T_{p\max} - Q_p^A)$ show that the analyzed process of ternary fission has the virtual character.

As can be seen from Figs. 6–7 the dependences $W_{pf}^{A}(T_p)$ from T_p for the spontaneous and induced ternary fission of the compound nuclei ^{236}U and ^{252}Cf with emission ^{2}H turn out to be close for all CFN considered.

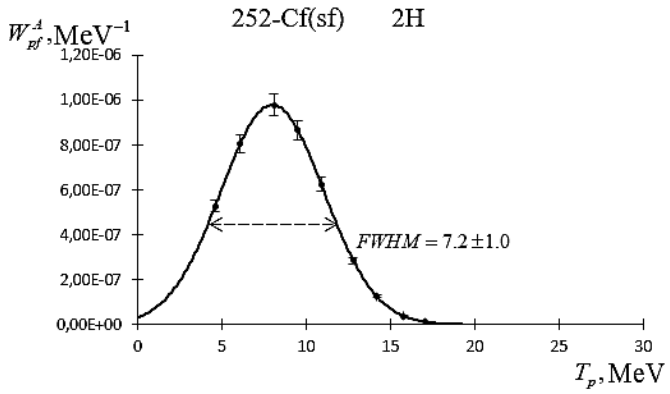

Fig. 6. The dependence $W_{pf}^{A}(T_p)$ for the spontaneous fission of the compound nucleus ^{252}Cf with emission ^{2}H.

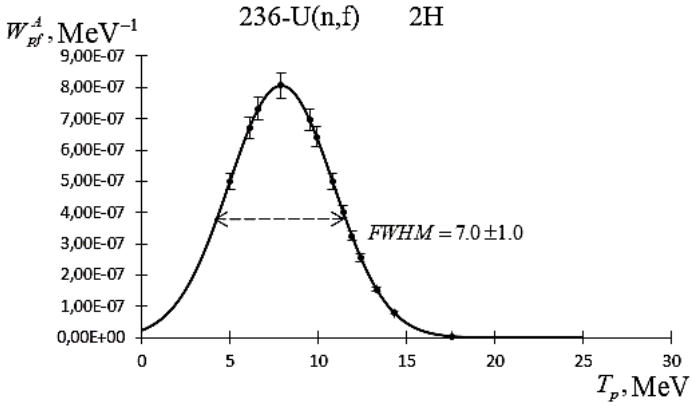

Fig. 7. The dependence $W_{pf}^{A}(T_p)$ for the induced fission of the compound nucleus ^{236}U with emission ^{2}H.

From Figs. 6–7 it can be seen that for both spontaneous and induced fission of CFN with emission ^{2}H such characteristics as width at half maximum *FWHM* and forms of energy distribution are close.

The experimental angular distributions of ^{2}H for all CFN [19–20] have the equatorial character with the maximum close to θ = 90°, what could be related with the emission of ^{2}H from the neck of the prescission configuration of CFN. Confirmation of this fact can be found in [27] for the spontaneous fission of the ^{252}Cf nucleus.

7. Spontaneous and induced ternary nuclear fission with the emission of prescission ^{3}H

When using experimental data for spontaneous (sf) and induced (n,f) ternary fission with the emission of *p*-particle as ^{3}H from CFN nuclei ^{244}Cm, ^{246}Cm [23], and ^{250}Cf, ^{252}Cf [24] the characteristics of these processes were calculated.

Table 4. Characteristics of spontaneous (sf) and induced (n,f) ternary fission of CFN with the emission of ^{3}H

Compound nucleus	δ_{pf} ×10^{-4}		$T_{p\max}$ (MeV)		Q_p^A (MeV)	r_{neck} (fm)	ω_p ×10^{-4}	
	(sf)	(n,f)	(sf)	(n,f)			(sf)	(n,f)
^{244}Cm	2.0	2.0	8.1	8.2	–11.1	2.5	0.9	0.9
^{246}Cm	1.7	1.9	8.1	8.4	–12.3	2.5	0.9	1.0
^{250}Cf	2.1	2.1	8.3	8.5	–9.8	2.5	0.7	0.8
^{252}Cf	1.9	2.2	8.6	8.5	–9.3	2.5	0.8	0.8

As can be seen from Table 4 for all considered CFN the yields δ_{pf} of ^{3}H are close to each other as for spontaneous as well induced fission: $1.7\times10^{-4} \le \delta_{pf} \le 2.2\times10^{-4}$. The analogous situation is realized for the probabilities of ^{3}H formation ω_p: $0.7\times10^{-4} \le \omega_p \le 1.0\times10^{-4}$. The noticeable positive values of differences $(T_{p\max} - Q_p^A)$ show that the analyzed process of ternary fission has the virtual character.

As can be seen from Figs. 8–10 the dependences $W_{pf}^A(T_p)$ from T_p for the spontaneous and induced ternary fission of the compound nuclei ^{250}Cf, ^{244}Cm and ^{246}Cm with emission ^{3}H turn out to be close for all CFN considered.

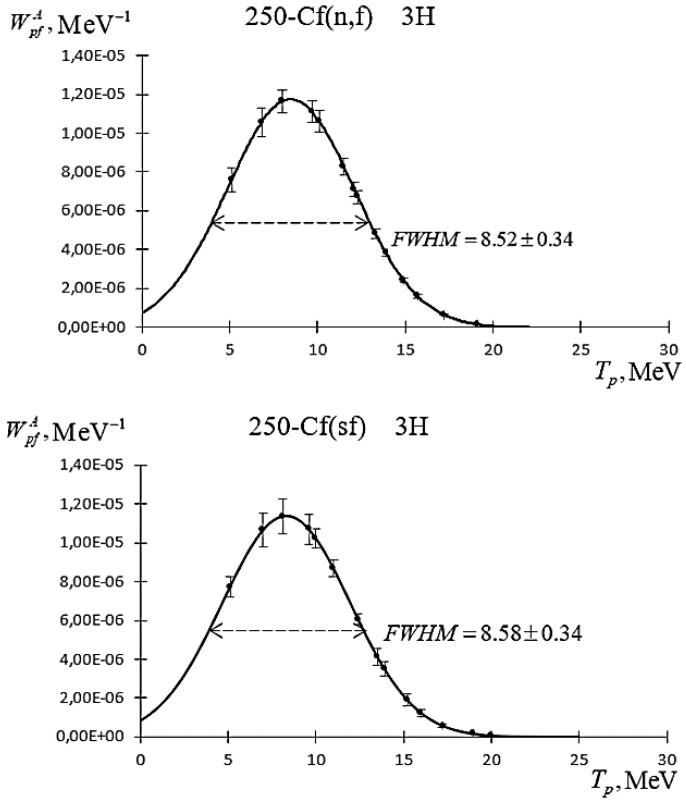

Fig. 8. The dependences $W_{pf}^A(T_p)$ for the induced and spontaneous fission of the compound nucleus ^{250}Cf with emission ^{3}H.

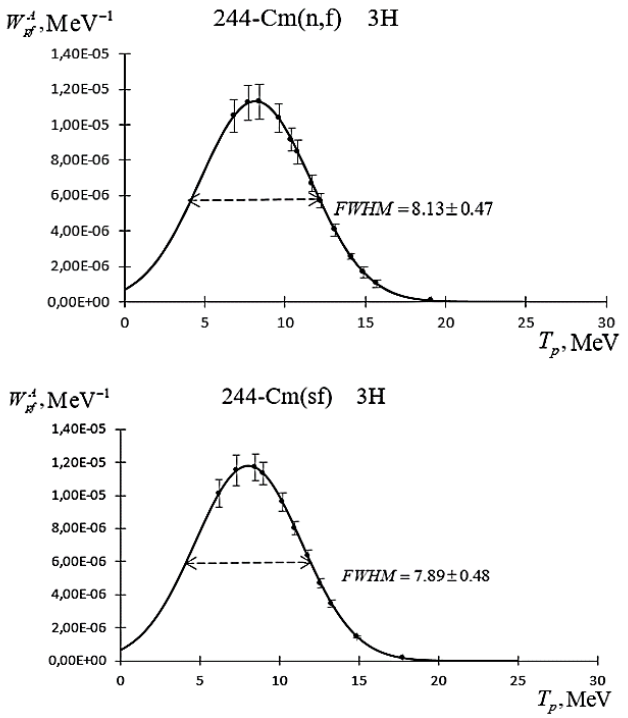

Fig. 9. The dependences $W_{pf}^{A}(T_p)$ for the induced and spontaneous fission of the compound nucleus ^{244}Cm with emission ^{3}H.

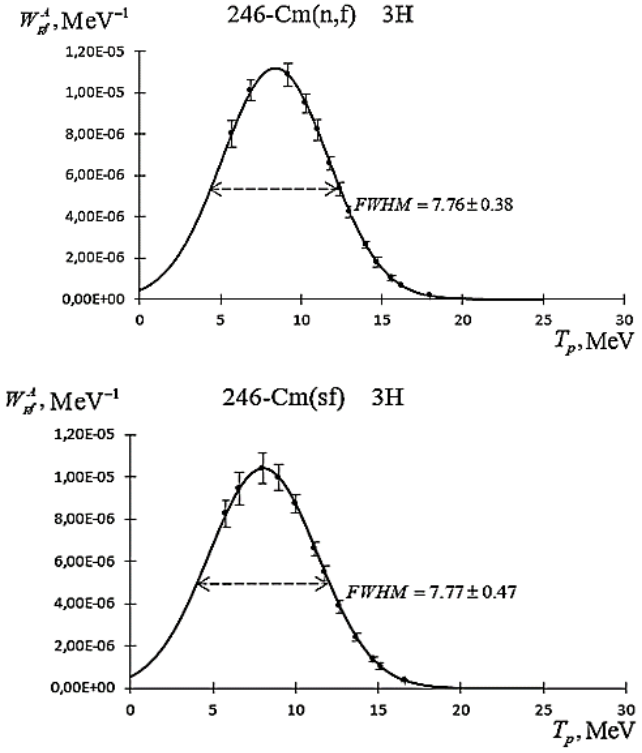

Fig. 10. The dependences $W_{pf}^{A}(T_p)$ for the induced and spontaneous fission of the compound nucleus ^{246}Cm with emission ^{3}H.

From Figs. 8–10 it can be seen that for both spontaneous and induced fission of CFN with emission ^{3}H such characteristics as width at half maximum *FWHM* and forms of energy distribution are close.

The experimental angular distributions of ^{3}H for all CFN [19–20] have the equatorial character with the maximum close to θ = 90°, what could be related with the emission of ^{3}H from the neck of the prescission configuration of CFN. Confirmation of this fact can be found in [26] for the spontaneous fission of the ^{252}Cf nucleus.

8. Spontaneous and induced ternary nuclear fission with the emission of prescission ^{6}He

When using experimental data for spontaneous (sf) and induced (n,f) ternary fission with the emission of *p*-particle as ^{6}He from CFN nuclei ^{250}Cf and ^{252}Cf [24] the characteristics of these processes were calculated.

Table 5. Characteristics of spontaneous (sf) and induced (n,f) ternary fission of CFN with the emission of ^{6}He

Compound nucleus	δ_{pf} ×10^{-5}		$T_{p\max}$ (MeV)		Q_p^A (MeV)	r_{neck} (fm)	ω_p ×10^{-3}	
	(sf)	(n,f)	(sf)	(n,f)			(sf)	(n,f)
^{250}Cf	8.0	7.0	10.6	11.0	–5.91	2.5	2.6	2.4
^{252}Cf	7.7	7.6	11.2	10.9	–4.18	2.5	2.5	2.2

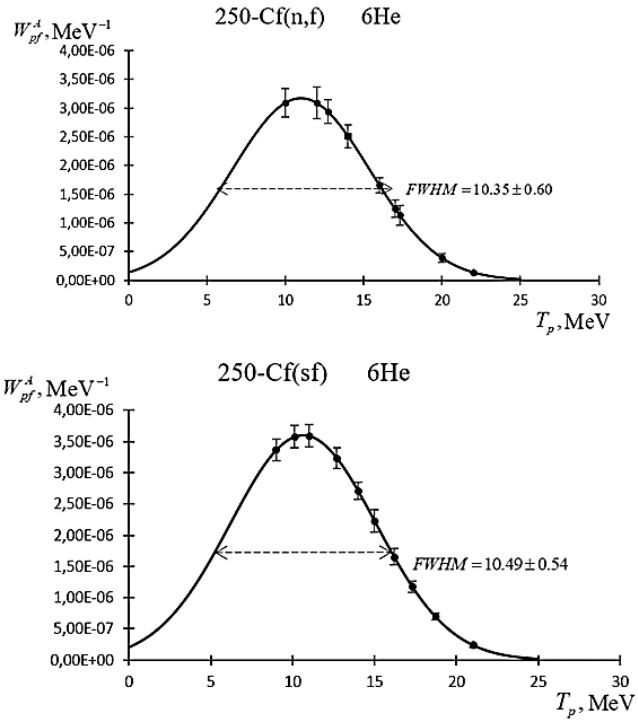

Fig. 11. The dependences $W_{pf}^{A}(T_p)$ for the induced and spontaneous fission of the compound nucleus ^{250}Cf with emission ^{6}H.

As can be seen from Table 5 for all considered CFN the yields δ_{pf} of ^{6}He are close to each other as for spontaneous as well induced fission: $7.0\times10^{-5} \le \delta_{pf} \le 8.0\times10^{-5}$. The analogous

situation is realized for the probabilities of ^{6}He formation ω_p: $2.2\times10^{-3} \le \omega_p \le 2.6\times10^{-3}$. The noticeable positive values of differences $(T_{p\max} - Q_p^A)$ show that the analyzed process of ternary fission has the virtual character.

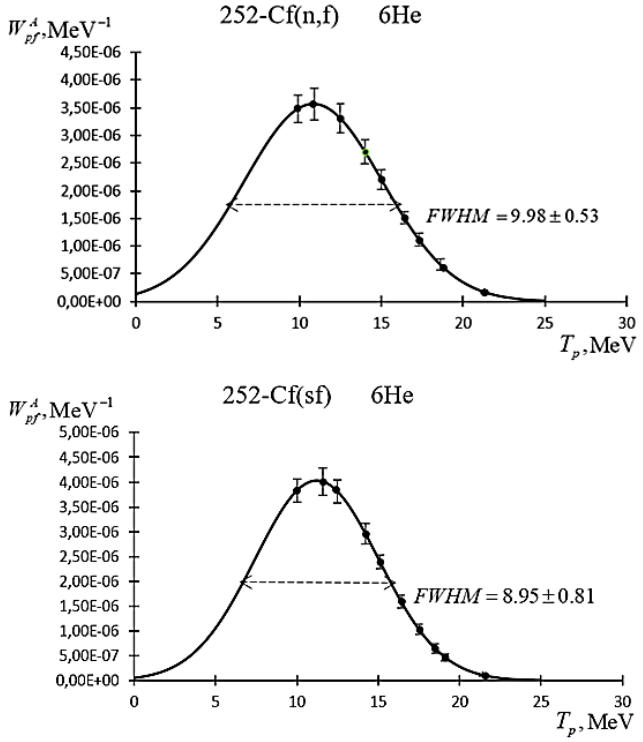

Fig. 12. The dependences $W_{pf}^A(T_p)$ for the spontaneous and induced fission of the compound nucleus ^{252}Cf with emission ^{6}He.

As can be seen from Figs. 11–12 the dependences $W_{pf}^A(T_p)$ from T_p for the spontaneous and induced ternary fission of the compound nuclei ^{250}Cf and ^{252}Cf with emission ^{6}He turn out to be close for all CFN considered.

From Figs. 11–12 it can be seen that for both spontaneous and induced fission of CFN with emission ^{6}He such characteristics as width at half maximum *FWHM* and forms of energy distribution are close.

The experimental angular distributions of ^{6}He for all CFN [19–20] have the equatorial character with the maximum close to $\theta = 90^{o}$, what could be related with the emission of ^{6}He from the neck of the prescission configuration of CFN. Confirmation of this fact can be found in [26] for the spontaneous fission of the ^{252}Cf nucleus.

9. Spontaneous and induced ternary nuclear fission with the emission of prescission neutrons

It is well known [11] that in the spontaneous and low-energy induced (by thermal neutrons) binary fission of actinide-nuclei the neutrons *n* with short characteristic escape times $\tau \le 10^{-4}$ s appear. The number of these neutron, normalized by their yield δ_{nf}, are determined by the normalized sum evaporated neutrons n_{ev} emitted from fission fragments, fully accelerated by their mutual Coulomb field, and prescission neutrons n_{pr}, emitted from prescission config-

urations of FN at times close to the moment of its scission into fission fragments. The angular and energy spectrum $n(T_n, \theta_n)$ of indicated neutrons n, where T_n and θ_n are the asymptotic kinetic energies of the emitted neutron and the angle between the directions of neutron emission and light fission fragment, can be presented as

$$n(T_n, \theta_n) = n_{pr}(T_n, \theta_n) + n_{ev}(T_n, \theta_n). \quad (11)$$

Experimental spectrum $n(T_n, \theta_n)$ are found for the spontaneous binary fission of the ^{252}Cf in [28, 29] and for neutron-induced binary fission of ^{233}U and ^{235}U in [29, 30]. Theoretical spectrum $n_{ev}(T_n, \theta_n)$ of evaporation neutrons can be calculated using the presentation [28]. The spectrum of prescission neutrons $n_{pr}(T_n, \theta_n)$ can be calculated using formula (11) with experimental values $n(T_n, \theta_n)$ and theoretical values $n_{ev}(T_n, \theta_n)$. The typical angular dependence of $n_{pr}(\theta_n)$ for the induced fission of the nucleus-target ^{233}U by thermal neutron with formation of CFN ^{234}U [29,30] shown on Fig. 13.

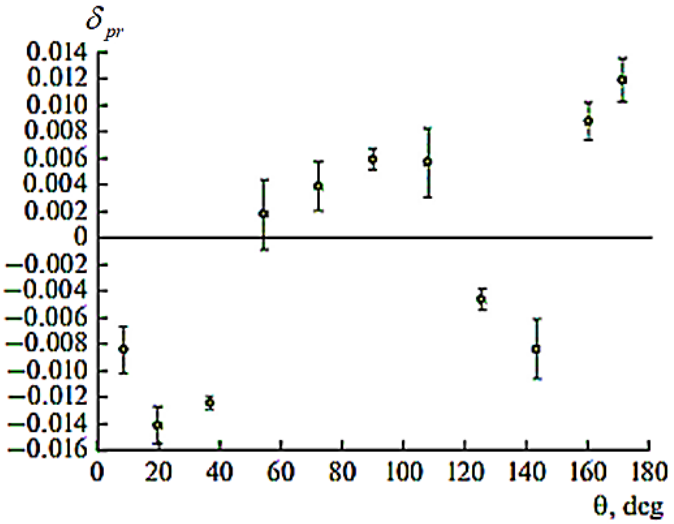

Fig. 13. Integral angular distribution prescission neutrons for CFN ^{234}U.

As can be seen from Fig. 13, the values of $n_{pr}(\theta_n)$ for certain angles θ turned out to be negative, which is physically impossible. This testifies to the inaccuracy of the formulas [28–31] used to calculate the evaporation spectra of neutrons. Therefore, the angular distributions of prescission neutrons calculated using formula (11) were corrected by throwing away the negative values of $n_{pr}(\theta_n)$ obtained in the calculations [28–31] and by conservation $n_{pr}(\theta_n)$ only for the angular range close to $\theta = 90°$.

Table 6. Characteristics of ternary fission of CFN with the emission of n_{pr}

Compound nucleus	δ_{pr} $\times 10^{-2}$	Angular range	$T_{p\max}$ (MeV)	Q_p^A (MeV)
^{233}U (n,f)	1.5	$54.5^o \le \theta \le 107.8^o$	0.5	-6.8
^{235}U (n,f)	1.8	$54.5^o \le \theta \le 107.8^o$	0.5	-6.5
^{252}Cf (sf)	2.0	$72.2^o \le \theta \le 107.8^o$	0.6	-6.2

As it can be seen from Table 6, where characteristics of spontaneous (sf) and induced (n,f) ternary fission with the emission of prescission neutrons n_{pr} from CFN nuclei ^{234}U [29, 30], ^{236}U [29, 30] and ^{252}Cf [28, 29] are presented, for all considered CFN the yields δ_{pr} for prescission neutrons are close for spontaneous and induced fission $1.5\times10^{-2} \le \delta_{pr} \le 2.0\times10^{-2}$. The noticeable positive values of differences $(T_{p\max} - Q_p^A)$ show that the analyzed process of ternary fission has the virtual character [4].

Figs. 14–15 demonstrate the corrected energy distributions of prescission neutrons n_{pr} for spontaneous fission of the ^{252}Cf nucleus [29] and induced fission of ^{235}U [30], respectively.

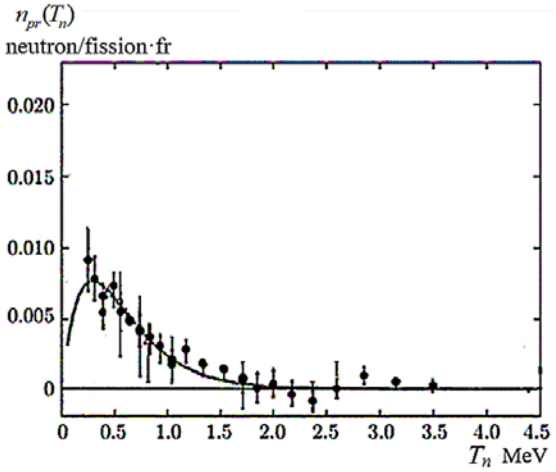

Fig. 14. Experimental energy distribution $n_{pr}(T_n)$ for spontaneous fission of the ^{252}Cf .

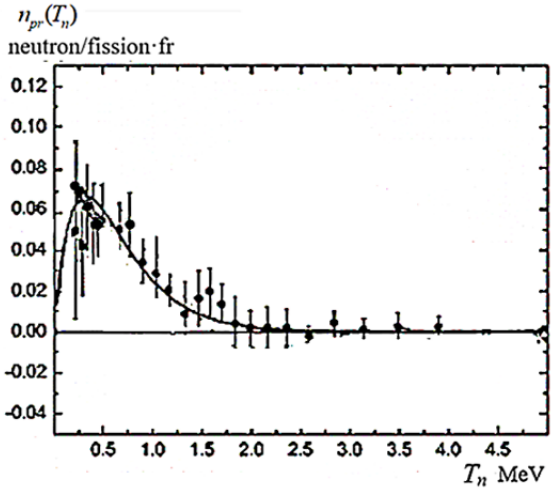

Fig. 15. Experimental energy distribution $n_{pr}(T_n)$ for induced fission of the ^{235}U.

From Figs. 14–15 it can be seen that for both spontaneous and induced fission of CFN with emission n_{pr} the energy distributions are close.

9. Conclusion

Based on the results obtained in this paper it can be concluded that for spontaneous and induced ternary fission the emission processes for prescission particles ^{1}H, ^{2}H, ^{3}H, ^{6}He and n_{pr} are similar to the analogous process for prescission α-particles.

Table 7. Characteristics of spontaneous (sf) and induced (n,f) ternary fission of CFN with the emission of prescission particles

Emitted particle p	δ_{pf}		$T_{p\max}$ (MeV)	Q_p^A (MeV)	ω_p	
	(sf)	(n,f)			(sf)	(n,f)
α	2.6×10^{-3}	2.2×10^{-3}	16	+6	2.6×10^{-2}	2.4×10^{-2}
^{1}H	4.6×10^{-5}	4.0×10^{-5}	8	–7	8.0×10^{-4}	6.0×10^{-4}
^{2}H	1.5×10^{-5}	1.2×10^{-5}	8	–9	5.0×10^{-4}	4.5×10^{-4}
^{3}H	1.9×10^{-4}	2.05×10^{-4}	8	–10	0.8×10^{-4}	0.9×10^{-4}
^{6}He	7.9×10^{-5}	7.3×10^{-5}	10	–6	2.6×10^{-3}	2.3×10^{-3}
n_{pr}	1.7×10^{-2}	2.0×10^{-2}	0,5	–6	-	-

From the Table 7, where the averaged values of yields δ_{pf}, of probabilities of formation ω_p, of maximal kinetic energies T_{pmax} of third particles p and of p-decay heats Q_p^A of CFN (A) for spontaneous and induced ternary fission with emission of all analyzed previously prescission particles p are presented, it can be obtained the following conclusions.

1. Birth processes for all prescission particles have virtual character, because differences $(T_{p\max} - Q_p^A)$ have noticeable positive values: 10 MeV for α-particles, (15–18) MeV for ^{1}H, ^{2}H, ^{3}H, ^{6}He and 6.5 MeV for prescission neutron. These differences are subtracted from the kinetic energy of fragments the binary fission of intermediate nuclei.

2. The values of energies $T_{p\max}$, yields δ_{pf} and probabilities of formation ω_p are close for each group of prescission particles in spontaneous and induced ternary fission of nuclei, since the excitation energy $|B_n|$ of CFN for the absorption of thermal neutron by the target-nucleus does not participate in the formation of the kinetic energy of prescission particles, but transforms to the excitation energy of binary fission fragments.

3. The yields δ_{pf} of prescission particles p have maximum values for prescission neutrons 1.85×10^{-2}, and then decrease to 2.4×10^{-3} for α-particles, to 2.0×10^{-4} for ^{3}H and then become less than 1.2×10^{-5} for ^{1}H, ^{2}H and ^{6}He. Similar changes occur for the formation probabilities ω_p calculated for all prescission particles, except for prescission neutrons.

Bibliography

1. A.I. Akhieser and V.B. Berestetsky, Quantum electrodynamics (Fizmatgiz, Moscow, 1959).
2. S.G. Kadmensky, U.V. Ivankov, Phys. Atom. Nucl. **77**. 1019 (2014); **77**. 1532 (2014).
3. S.G. Kadmensky, A.O. Bulychev, Bull. Russ. Acad. Sci., Phys. **79**. 872 (2015); **80**. 1009 (2016).
4. S.G. Kadmensky, L.V. Titova, D.E. Lyubashevsky, Phys. Atom. Nucl. **83**. 581 (2020).
5. V.I. Goldansky, JETP. **39**. 497 (1960); UFN 87. 255 (1965).
6. L.A. Sliv, JETP, **20**. 1035 (1950).
7. J.Suhoen, O.Civitareze, Phys. Rep. 300, 123 (1998).

8. V.I. Tretyak, Double beta decay: history and current status, Institute for Nuclear Research. (2014).
9. D. E. Lyubashevsky, Bull. Russ. Acad. Sci., Phys. **84**. 1406 (2020).
10. S.G. Kadmensky, L.V. Titova, Bull. Russ. Acad. Sci., Phys. **85**. 732 (2021).
11. A. Bohr, B. Mottelson Nuclear Structure (Benjamin, New York, 1974), V.1, V2.
12. C.F. Weizssacker, Zs. f. Phys. **96**. 431 (1935).
13. V.M. Strutinsky, JETP. **37**. 613 (1960).
14. V.M. Strutinsky, Nucl. Phys. **3**. 614 (1965).
15. E.P. Wigner, Ann. Math. **62**. 548 (1955); **65**. 203 (1958); **67**. 325 (1958).
16. S.G. Kadmensky, V.P. Markushev, V.I. Furman, Nucl. Phys. **35**. 300 (1982).
17. S.G. Kadmensky, Nucl. Phys. **65**. 1833 (2002).
18. S.G. Kadmensky, L.V. Titova, P.V. Kostryukov, Bull. Ras. Phys. **82**. 1299 (2015).
19. M. Mutterer, J.P. Theobald, Dinuclear Decay Modes. Bristol: IOP Publ., Chap. 1. 12. (1996).
20. M. Mutterer, Yu.N. Kopatch, P. Jesinger et al., Nucl. Phys. A. **738**. 122 (2004).
21. O. Serot, N. Carjan, C. Wagemans, Eur. Phys. J. A. **8**. 187 (2000).
22. S.G. Kadmensky, V.I. Furman, Alpha decay and related nuclear reactions, M.: Energoatomizdat, 1985.
23. S. Vermote, C. Wagemans, O. Serot, Nucl. Phys. A. **806**. 1 (2008).
24. S. Vermote, C. Wagemans, O. Serot, Nucl. Phys. A. **837**. 176 (2010).
25. O. Serot, C. Wagemans, J. Heyse AIP Conf. Proc. **769**. 857 (2005).
26. Yu.N.Kopatch, M.Mutterer Phys. Rev. C. **65.** P. 044614-1, (2002).
27. G. M. Raisbeck, T.D. Thomas, Phys. Rev. **172**. 1272 (1968).
28. J. Chwaszczewska, Phys. Lett. **24B**. 87 (1967).
29. A.S. Vorobyev et al., JETF. **152**. 730 (2017).
30. A.S. Vorobyev et al., Bull. Russ. Acad. Sci., Phys. **82**. 1373 (2018).
31. A.S. Vorobyev et al., EPJ Web of Conferences. **239**. 05008 (2020).
32. R. Capote et al., Nucl. Data Sheets. **131**. 1 (2016).